JOURNAL OF CATALYSIS 141, 566–582 (1993)

Hydrogenation of 1-Butene and 1,3-Butadiene Mixtures over Pd/ZnO Catalysts

A. SARKANY,* Z. ZSOLDOS,* B. FURLONG,† J. W. HIGHTOWER,† AND L. GUCZI*

*Institute of Isotopes of the Hungarian Academy of Sciences, P.O. Box 77, H-1525 Budapest, Hungary; and †Department of Chemical Engineering, Rice University, Houston, Texas 77251-1892

Received July 16, 1992; revised January 21, 1993

Several palladium catalysts supported on ZnO with different loadings and dispersions have been prepared, characterized, pretreated, and tested for the selective hydrogenation of small amounts of 1,3-butadiene in 1-butene. Hydrogen treatment at temperatures above 423 K caused a marked decrease in catalytic activity and a simultaneous increase in selectivity for reduction of butadiene primarily to olefins. Such treatment also caused partial reduction of the ZnO support which resulted in the formation of PdZn intermetallic phases (XRD results). XPS measurements suggested that the Pd crystallites were "decorated" with reduced Zn metal which significantly decreased the availability of the Pd adsorption sites, as determined by hydrogen and carbon monoxide chemisorption. Alternate oxidation and temperature-programmed reduction cycles could distinguish between the formation of $(PdO)_x$ and oxidation of the reduced Zn. Even though the overall activity was decreased after high-temperature exposure to hydrogen, the turnover frequency for the smaller number of active sites remained virtually unchanged. Moreover, the activation energy and reaction orders were not altered. High-temperature reduction also decreased the *trans*/*cis*-2-butene ratio formed from the butadiene; this may reflect slow interconversion between the *syn* and *anti* conformation of the 1,3-butadiene adsorbed on the Zn-decorated surface. These experiments have identified some of the important roles of the support and pretreatment conditions on the performance of such catalysts.

INTRODUCTION

It is well established that support materials play an essential role in the catalytic activity of highly dispersed metals (*1–3*). Particle size and support effects are interdependent and can contribute significantly to the surface composition and textural properties of supported catalysts (*4*). Pretreatment conditions, especially temperature of reduction, lead to SMSI states with titania, vanadia, and other reducible oxides (*3*). While the nature of the SMSI state has been the subject of systematic investigations, apparently no unifying theory exists (*4, 5*).

Because ZnO exhibits multifunctional behavior and has interesting promoting effects, it has been the subject of considerable attention as a versatile catalyst support. Zn atoms or ions increase the rate of hydroformylation and improve olefin selectivity in CO hydrogenation over Rh catalysts (*6, 7*). XPS and reduction studies have confirmed the presence of Zn^0 in these systems (*7, 9*). Ichikawa (*10*) reported unusually high selectivities >90% for methanol formation during CO/H_2 reaction over ZnO. It has been suggested that Lewis acidity of ZnO facilitates migratory insertion of CO or that Rh(I) species are stabilized by ZnO (*7*). Hydrogen treatment of Pt/ZnO catalysts enhances activity for the water gas shift reaction (*11*). The increase in methanation activity above 473 K (*12, 13*) was attributed to enhanced electron density on Pt sites. Electron microscopy indicated morphological changes, e.g., spherical particles have taken on a shape resembling flying saucers (*14*), and formation of PdZn and PtZn intermetallics have also been observed (*12, 14*).

Investigations directed towards understanding the effect of Zn^0 or Zn ions as ad-

0021-9517/93 $5.00

ditives in hydrogenations (*15*) are scarce, although ZnO is known to hydrogenate and isomerize alkenes at moderate temperatures (*16–21*). Zn^{+2} ions added in form of acetate to Pt improve the selectivity of hydrogenation of α,β-unsaturated aldehydes (*22*). Modification of Pd by $CdSO_4$ and $ZnSO_4$ increases the selectivity of olefinic carbinols formed from acetylenic compounds (*23*). The surface composition of the catalysts and the oxidation state of the Zn were not investigated in these studies.

This paper deals with the catalytic properties of Pd/ZnO catalysts in hydrogenation of 1,3-butadiene and 1,3-butadiene/1-butene mixtures. The main objective is to investigate the effect of reduction on the rate and selectivity of hydrogenation. Considering the red shift of CO stretching frequency observed after reduction treatment of Pt/ZnO (*12*, *13*), one might expect that Zn atoms decorate Pd sites to exert geometric and ligand effects which influence the competitive adsorption of 1,3-butadiene and 1-butene on Pd sites. To some extent the effect of Zn atoms might be compared to nitrogen bases which are electron donors known to increase the selectivity of competitive hydrogenation of 1-butyne in 1-butene (*24*, *25*) by influencing the strength of complexation. The geometric and electronic effects of Zn are likely to influence the availability of surface hydrogen and might hinder adsorption of alkene as has been observed with Pd–Pb, Pd–Ag, Pd–Cu, and Pd–Au bimetallic catalysts in hydrogenation of acetylene–ethylene mixtures (*26*, *27*). The present work is also designed to collect data on the reduction of ZnO similar to those already observed in the formation of bimetallic particles over Pd/ZnO similar to those already reported on Pt/ZnO at 493 K (*12*, *13*).

EXPERIMENTAL

Catalyst Preparation

Prior to catalyst preparation, the ZnO support (Kadox 25) was air treated at 698 K. Seven catalysts prepared with different Pd precursors and loadings are listed in Table 1.

TABLE 1

Catalysts Prepared

Support: ZnO, Kadox 25, S(BET) = 7.3 m^2g

Sample	Precursor	Pd (m%)	BET[a]	CO[b]	H_s(HT)	H_b/Pd_b[c]	D(CO)%[d]
A	$PdCl_2$	0.3[f]	6.8(6.3)	3.5	3.5	0.68	12.3
B	$[Pd(NH_3)_4]Cl_2$	0.5[f]	6.9(6.1)	6.2	5.5	0.66	13.1
C	$PdCl_2$	2.5[f]	6.8		21.9	0.72	9.3[e]
D	$Pd(C_5H_7O_2)_2$	0.1	7.1(6.8)	7.4	6.3	0.61	78.4
E	Pd+ZnO	8.5	6.6(4.7)	22.2	21.0	0.74	2.7
F	Pd+ZnO	4.4	—	—	—	—	—
G	$[Pd(NH_3)_2](NO_2)_2$	0.5	6.9(6.7)	30.1	24.1	0.69	63.9

[a] The value in parenthesis after reduction at 673 K for 30 min in 46.6 kPa H_2. C constant varied between 47.5 and 67.8.

[b] In μmol/g cat. CO chemisorption determined from CO titration of Pd_s–O, sample reduced in diluted N_2H_4 and O_2 treated at 393 K; H_s(HT) chemisorbed hydrogen (μmol/g cat.) determined by hydrogen titration after oxidation at 393 K.

[c] H_b/Pd_b hydrogen dissolved in the bulk, Pd_s was taken from hydrogen titration.

[d] Dispersion in %, $CO/Pd_s = 1$ and $H_s/Pd_s = 1$.

[e] From hydrogen chemisorption.

[f] Samples A, B, and C were NH_4OH washed.

(A) 0.3 wt% Pd/ZnO was prepared from a solution of $PdCl_2$ dissolved in acetone containing a few drops of 0.1 *N* HCl to facilitate solubility of the $PdCl_2$. The support was mixed with the solution and dried at 393 K in air for 14 h.

(B) 0.5 wt% Pd/ZnO was prepared from $Pd(NH_3)_4Cl_2$ dissolved in dilute NH_4OH. After the support was added, the sample was dried overnight at 393 K and decomposed at 573 K in air.

(C) 2.5 wt% Pd/ZnO was prepared by careful mechanical mixing of a slurry containing $PdCl_2$ and ZnO in presence of acetone.

(D) Preparation of a 0.1 wt% Pd/ZnO involved impregnating ZnO with Pd(II)acetylacetonate dissolved in benzene. The catalyst was dried at 373 and decomposed at 523 K in air.

(E) and (F) 8.5 and 4.4 wt% Pd/ZnO catalysts were made by mixing PdO and ZnO mechanically. PdO powder was prepared from $Pd(NO_3)_2$ and had a BET surface area of 15.2 m^2/g.

(G) 0.5 wt% Pd/ZnO was prepared from a solution of $[Pd(NH_3)_2](NO_2)_2$ dissolved in diluted NH_4OH and acetone. After drying at 353 K in air the sample was reduced in H_2 at 383 K and O_2-treated at 433 K for 30 min.

Catalyst Characterization

Catalysts B (0.5% Pd), E (8.5% Pd), and C (2.5% Pd) were characterized by XRD to estimate metal particle size and to measure changes in the catalyst composition following reduction at elevated temperatures. Powder diffractograms (Cu $K_{\alpha 1}$, λ = 0.15405 nm) were measured in a Guinier camera equipped with a curved quartz monochromator.

X-ray fluorescence was used to determine metal concentrations following the reduction in N_2H_4 and chlorine removal with NH_4OH solution.

Both hydrogen chemisorption and absorption were measured under dynamic conditions by frontal analysis of H_2 adsorption (*28*). In determining the concentration of surface sites Pd_s, a low hydrogen pressure of 49.98 Pa was applied to avoid hydride phase formation (*29–31*). The formation of both surface and hydride phases was measured at the higher pressure of 4.748 kPa H_2 following the chemisorption at 49.98 Pa H_2; the H_b/Pd_t and H_b/Pd_b ratios were then calculated by assuming $Pd_b = Pd_t - Pd_s$ (subscripts b, t, and s refer to bulk, total, and surface atoms, respectively) (*31*).

H_2 sorption, CO, and O_2 chemisorptions and titrations were performed at 293 K unless otherwise stated. The usual set of stochiometries has been considered (*29, 30*). By making gravimetric measurements (Sartorius 4102 type microbalance), hydrogen absorption, O_2, and CO chemisorptions were determined after reduction. From the weight loss caused by oxygen removal, the Zn^0/Pd ratio was calculated.

Reducibility of the catalyst precursors was followed by temperature programmed reduction (TPR) in a flow system with 10 v% H_2/Ar. The technique involved flowing the H_2/Ar mixture over catalyst samples at ambient temperature for 30 min and then linearly ramping the temperature at 20 K/min up to 950 K. Peak areas were determined, and moles of oxygen removed were calculated after calibration experiments. The same experimental setup was used for temperature programmed desorption of hydrogen in Ar with a heating rate of 20 K/min.

XPS measurements were carried out with a KRATOS ES-300 type ESCA machine. X-ray patterns were generated with an aluminum anode ($K_{\alpha 1,2}$ = 1486.6 eV, 150W) with the hemispherical analyzer working in a Fixed Retarding Ratio (FRR) mode. *In situ* sample reduction was carried out sequentially in flowing H_2 in a small reaction chamber attached directly to the ESCA machine. This arrangement allowed transfer of the reduced samples into the analyzing chamber without exposure to air. During analysis the pressure in the Sample Analyzing Chamber (SAC) did not exceed 10^{-6} Pa.

All binding energies (B.E.) were referenced to the C 1*s* peak (284.8 eV $B.E._{ref}$) as an internal standard.

Catalytic Reactions

The catalysts were tested for selective hydrogenation activity by passing 1,3-butadiene/H_2 and 1-butene/1,3-butadiene/H_2 mixtures at atmospheric pressure through a small tubular flow reactor (*32*) containing 0.0005–0.05 g of catalyst. The total flow rate was maintained in the range of 30–100 cm^3/min with MKS mass flow controllers. Typical composition of the inlet was 1.9 v% H_2, 0.25 v% 1,3-butadiene, 2.25 v% 1-butene; the remaining 95.6% was high purity N_2. Product selectivities for *n*-butane (SnB), 1-butene (S1B), *trans*-2-butene (St2), and *cis*-2-butene (Sc2) were calculated as the moles of that product formed divided by the moles of butadiene consumed (*32*). A positive selectivity for 1-butene indicates more 1-butene in the product than was present in the inlet stream, i.e., a net production of that species. Conversion refers to butadiene consumed.

Additional experiments with 5.0 kPa butadiene were performed in a static circulation system (volume = 187 cm^3).

Products were separated by GLC using a 20% BMEA or *n*-octane/Porsail-C column at 298 K.

RESULTS

Adsorption

The BET area of the supported samples presented in Table 1 are comparable to values measured by Dent and Kokes (*16, 18*). Hydrogenation or oxidation treatments in the 673–773 K range caused slight sintering of the support as indicated by a decrease of the surface area (column 4, values in parentheses). The prepared catalysts listed in Table 1 were reduced at 393 K and oxidized at 453 K prior to hydrogen titration and CO chemisorption. The chemisorption results in Table 1 (later referred to as H_o or CO_o values) were compared with those obtained after H_2 reduction at elevated temperatures. With catalysts A, B, and C the results refer to samples which were NH_4OH washed (0.1 N) after reduction treatment at 393 K. Samples in Table 1 can be divided into two groups: A, B, and E exhibit lower dispersions, D and G higher dispersions. The constancy of the H_b/Pd_b values in column 7 (average 0.68+/−0.04 for all samples) coupled with their insensitivity to dispersion confirms the bulk assignment (*31*). Of course, for very small crystallites (<25 Å) the bulk hydride phase would be expected to disappear.

Tables 2 and 3 show results obtained for samples C, D, and G when the following series of sequential experiments were performed. $H_s(A)$ and $O_s(A)$ (columns 2 and 3) represent surface sites determined by chemisorption of hydrogen and oxygen at ambient temperature after reduction treatment and desorption of hydrogen at 473–483 K. Oxygen chemisorption ($O_s(A)$, column 3) was followed by hydrogen and oxygen titrations [$H_s(T)$ and $O_s(T)$, columns 4 and 5]. H_s and O_s values represent surface concentrations assuming the usual stoichiometries.

TABLE 2

Oxygen and Hydrogen Adsorption (μmol/g cat.)

Pretreatment	$H_s(A)$	$O_s(A)$	$H_s(T)$	$O_s(T)$	$O_s(T)/O_s(A)$
Catalyst F, 0.5 wt% Pd/ZnO					
H_2/453 K (60 min)	3.53	13.65	10.11	9.97	0.73
H_2/543 K (10 min)	—	20.88	9.23	9.23	0.44
H_2/543 K	2.31	22.05	7.93	8.85	0.40
H_2/623 K	1.17	19.83	7.68	7.91	0.40
Catalyst D, 0.1 wt% Pd/ZnO					
H_2/423 K	1.31	4.18	3.33	3.22	0.77
H_2/543 K	0.61	5.26	3.43	3.36	0.64
H_2/600 K	0.38	5.33	3.11	3.03	0.56
H_2/650 K	0.27	4.24	1.56	1.23	0.29

Note. A: adsorption at 298 K (Surface hydrogen had been removed by TPD in Ar at 473–483 K). Reductions in 10.25 kPa H_2 for 30 min unless otherwise stated. $H_s(T)$: Hydrogen titration of Pd_s–O, where $2Pd_s\text{–}O + 1.5\ H_2 = Pd_s\text{–}H + H_2O$. $O_s(T)$: Oxygen titration of Pd_s–H, where $2Pd_s\text{–}H + 1.5\ O_2 = 2\ Pd_s\text{–}O + H_2O$. H_s and O_s in μmol of surface sites adsorbing H_s and O_s, respectively.

TABLE 3

Hydrogen and Oxygen Adsorption (μmol/g cat.)

Pretreatment	H_s(A)	O_s(A)	H_s(T)	O_s(T)	O_s(T)/O_s(A)
Catalyst C, 2.5 wt% Pd/ZnO (without NH_4OH treatment)					
H_2/383 K	3.7	—[a]	8.71	—	—
(10 min)		—[b]	10.6	—	—
H_2/380 K (55 min)	2.83	16.7	1.98	2.18	0.13
H_2/493 K	0.61	10.2	1.9	0.6	0.06
H_2/540 K (35 min)	0	3.1	0	0	—
H_2/628 K	0.002	0.8	0	0	—
ox 375–645 K red H_2/300 K	—	11.2	9.1	10.3	0.92
Catalyst C, 2.5 wt% Pd/ZnO (NH_4OH treated)					
H_2/423 K	6.02	10.3	7.8	10.1	0.98
H_2/451 K	5.8	13.5	11.3	10.8	0.8
(20 min)	—[c]	—	18.5	19.1	1.13
H_2/493 K	2.54	4.1	3.3	3.5	0.85
H_2/530 K	0.63	2.3	0.9	1.3	0.56
ox 657 K, red H_2/303 K	18.2	17.5	16.8	17.8	1.02
Catalyst A, 0.3 wt% Pd/ZnO (without NH_4OH treatment)					
H_2/461 K	0.06	0.98	0.15	—	
H_2/528 K	—	0.13	0.01	—	
Catalyst A, 0.3 wt% (Pd/ZnO (NH_4OH treated)					
H_2/493 K	0.14	2.8	1.2	0.8	
H_2/535 K	0.07	1.4	0.28	0.11	

Note. Reduction in 10.25 kPa H_2 for 30 min unless otherwise stated.

[a] Oxidation at 298 K, 6 min.

[b] Oxidation at 298 K, 61 min.

[c] Oxidation at 448 K, 20 min.

Upon reduction and TPD, the hydrogen chemisorption is suppressed significantly where the O_2 chemisorption actually increased (compare columns 2 and 3). As shown by column 4 part of the chemisorbed oxygen could be titrated by 49.98 Pa H_2 (dynamic frontal analysis) and the chemisorbed hydrogen (column 5) by oxygen. The values of O_2 chemisorption (O_s(A), column 3) and O_2 titration (O_s(T), column 5) were used to estimate an hypothetical Pd_s/(Pd+ZnO+Zn^+)$_s$ ratio on the surface. In the calculation it was assumed that ZnO (or Zn^+) formed in the course of hydrogenation is able to chemisorb oxygen in presence of Pd_s, but the Zn_s–O so formed cannot be titrated by H_2 at 298 K.

Increasing the reduction temperature decreases both the extent of hydride phase formation and the chemisorption of H_2 and CO (Tables 2 and 3 and Figs. 1–3). Figures 1 and 2 show the relative changes in H_2 chemisorption, $(H/H_o)_s$, and absorption, $(H/H_o)_b$, as functions of reduction temperature. For two samples, C and E, the $(H/H_o)_b$ ratios were determined from the area of the desorption peak at 353–383 K in a 9.98 kPa H_2/Argon stream.

With catalysts A, B, and C prepared with chlorine containing Pd compounds, the NH_4OH treatment exerts some effect on the chemisorption behavior. Without NH_4OH washing the oxygen uptake and the subsequent formation of hydrogen chemisorption sites are suppressed drastically above 473 K. The results with sample F (4.4 wt% Pd/ZnO) obtained in a gravimetric system are presented in Fig. 6. At higher

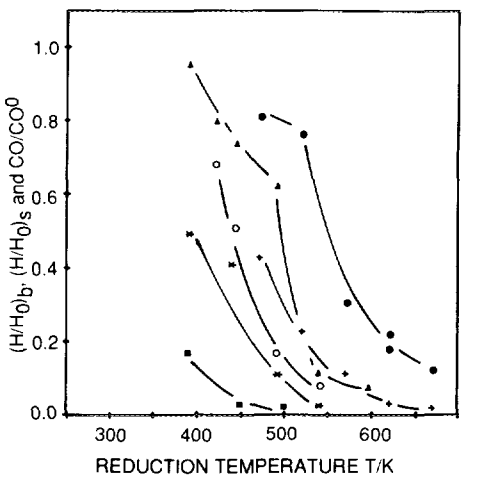

FIG. 1. Variation of the H_2 chemisorption $(H/H_o)_s$, CO chemisorption CO/CO_o, and hydrogen absorption $(H/H_o)_b$ as a function of reduction treatment in H_2 (10.25 kPa H_2 for 20 min). Sample E (8.5 wt% Pd/ZnO): ●, $(H/H_o)_b$; +, $(H/H_o)_s$. Sample C (2.5 wt% Pd/ZnO, NH_4OH washed): ▲, $(H/H_o)_b$; *, $(H/H_o)_s$; ●, CO/CO_o. Sample C (2.5 wt% Pd/ZnO, $ZnCl_2$ not removed): ■, $(H/H_o)_s$. [Note: With catalyst C $(H/H_o)_b$ was determined from TPD in 10% H_2 in Ar.]

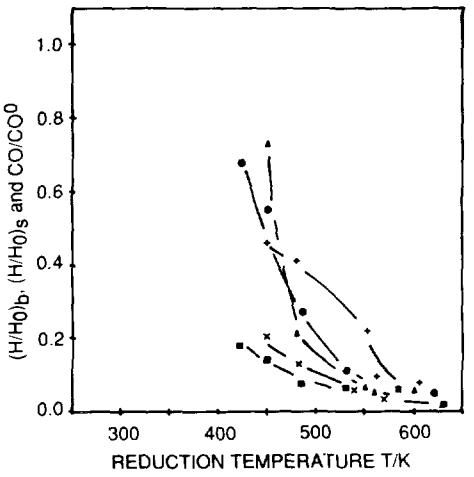

FIG. 2. Variation of the H_2 chemisorption $(H/H_o)_s$, CO chemisorption CO/CO_o, and hydrogen absorption $(H/H_o)_b$ as a function of reduction treatment in H_2 (10.25 kPa H_2 for 30 min). Sample D (0.1 wt% Pd/ZnO): ●, $(H/H_o)_b$; ■, $(H/H_o)_s$. Sample G (0.5 wt% Pd/ZnO): ▲, $(H/H_o)_b$; ×, $(H/H_o)_s$; +, CO/CO_o.

degrees of reduction, i.e., at large values of x, both hydrogen adsorption and CO chemisorption are decreased whereas O_2 chemisorption measured at 393 remains about constant or actually increases slightly.

Temperature-Programmed Reduction

Temperature-programmed reduction spectra are summarized in Figs. 4 and 5. Preliminary runs confirmed that PdO is reduced to metallic Pd at ambient temperatures. For sample F (curve 6 in Fig. 4, 4.4 Pd + ZnO) the features of the TPR curve are quite simple. Decomposition of the hydride phase in 10.25 kPa H_2 appears at 363 K and is followed by hydrogen consumption starting from about 523 K and reaching a maximum at 758 K. A similar curve was reported by Hong *et al.* (*14*) who observed a peak maximum at 700 K; their catalyst

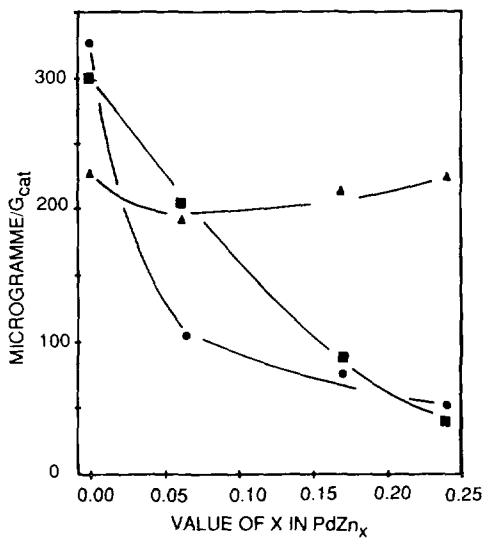

FIG. 3. Gravimetric measurements with catalyst F (4.4 wt% Pd/ZnO). ●, CO chemisorption; ▲, O_2 chemisorption; ■, H_2 absorption as a function of ZnO/Pd ratio. [CO (0.65 kPa) and H_2 (93 kPa H_2) adsorption at 293 K; O_2 (0.65 kPa) at 393 K.]

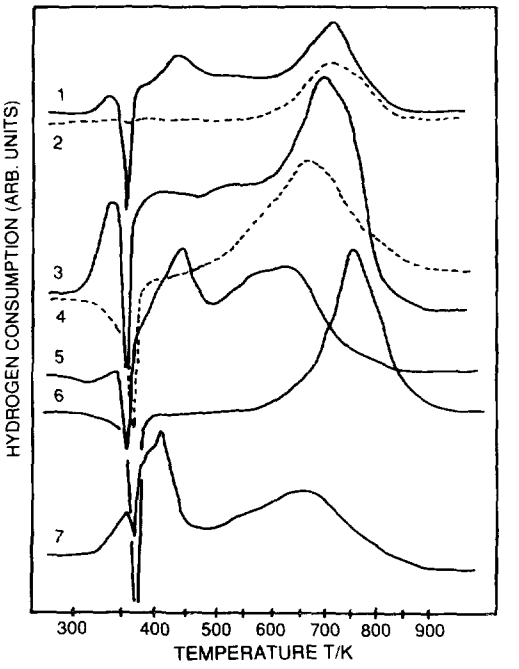

FIG. 4. Temperature-programmed reduction (20 K/min, 10% H_2/Ar, 38 ml/min): 1—catalyst B (0.5 wt% Pd/ZnO); 2—catalyst B prereduced at 503 K; 3—catalyst C (2.5 wt% Pd/ZnO) oxidized at 623 prior to reduction; 4—same as 3, but NH_4OH washed; 5—catalyst C reduced directly; 6—catalyst F (4.4 wt% Pd/ZnO); 7—catalyst A (0.3 wt% Pd/ZnO).

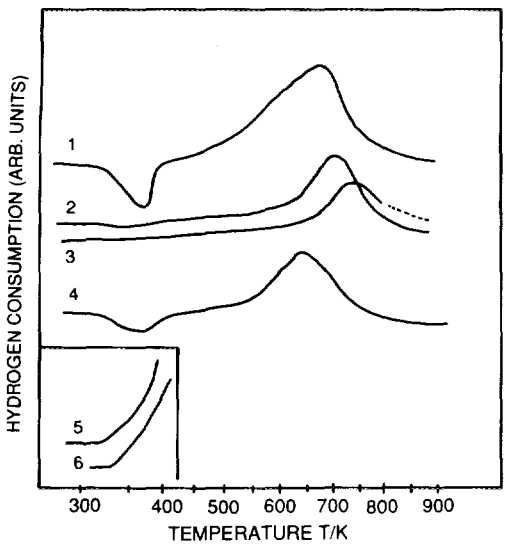

FIG. 5. Temperature-programmed reduction (20 K/min, 10% H_2/Ar, 38 ml/min): 1—catalyst G (0.5 wt% Pd/ZnO); 2—catalyst G prereduced at 473 K; 3—catalyst G prereduced at 573 K; 4—catalyst D (0.1 wt% Pd/ZnO); 5—reduction of catalyst G in 45 Pa H_2; 6—reduction of catalyst D in 45 Pa H_2.

was prepared from $Pd(NH_3)_4Cl_2$ by N_2H_4 reduction.

The presence of chlorine introduced by using $PdCl_2$ (sample A, curve 7 in Fig. 4; sample C, curves 3 and 5) and $Pd(NH_3)_4Cl_2$ (sample B, curve 1) influences the reduction behavior as indicated by hydrogen consumption. With chlorine-containing samples the onset of hydrogen uptake is at 323 K, and there is a continuous consumption of hydrogen up to 750 K interrupted with a negative hydride decomposition peak at 363 K. We attribute the hydrogen consumption at low temperatures to either (i) incomplete reduction of Pd^{+2} at 298 K or (ii) reduction of ZnO or $ZnCl_2$ at the Pd–support interface. Attempts were made to determine the amount of chlorine removed from the catalysts during the course of O_2 or H_2 treatments. Effluents were bubbled through a few cm^3 of H_2O and the pH or Cl^- concentrations were measured. The experiments indicated that chlorine left the catalysts only in the form of $ZnCl_2$ which sublimed from about 723 K (melting point 556 K) and condensed on the cold part of the reactor tube.

The effect of chlorine on the reducibility is clearly discernible if one compares the chlorine-containing samples with those which were N_2H_4-reduced and/or NH_4OH-washed (sample C, curves 3 and 4 in Fig. 4). Reduction of ZnO on the NH_4OH-washed samples gave a broad peak centered at about 623–673 K. These temperatures are lower than those observed with PdO+ZnO (sample E, curve 6 in Fig. 4) as a consequence of a more intimate contact between Pd particles and ZnO. Even lower reduction temperatures were observed in Fig. 5 for the more dispersed samples D (Pd $(acac)_2$) and E ($[Pd(NH_3)_2](NO_2)_2$); the reduction process in 0.13% H_2/Ar could be detected from about 353 K (insert in Fig. 5). With sample F (4.4 wt% Pd) prereduced at 323 K in 10.25 kPa, H_2 hydrogen consumption in 0.13% H_2/Ar started at 523 K.

The volume of hydrogen consumed at 723–773 K supports the formation of a PdZn phase as the Zn/Pd ratios calculated for catalysts C and E were 0.98–0.97 and 0.83–0.95, respectively. Catalysts G and D gave Zn^0/Pd values somewhat larger than unity (1.05–1.12).

TPD of Chemisorbed Hydrogen

TPD experiments indicated very limited desorption of hydrogen from the Pd/ZnO catalysts. Desorption of hydrogen from Samples D and G can be characterized by a broad peak at 363–383 K (typical results appear in Fig. 6, curves 5 and 6). Prior to TPD the samples were oxidized at 383 K and then hydrogenated at 298 K in 49.98 Pa H_2. A remarkable feature of these curves is that the hydrogen desorbed is only 3.5–5% of the hydrogen uptake observed by hydrogen titration at ambient temperature (Tables 1–3). The unrecovered chemisorbed hydrogen is likely consumed in reducing ZnO at the elevated temperatures. Hydrogenation of Sample G in 47 kPa H_2 at 536 and 627 K (after 30 min 47 kPa H_2 was re-

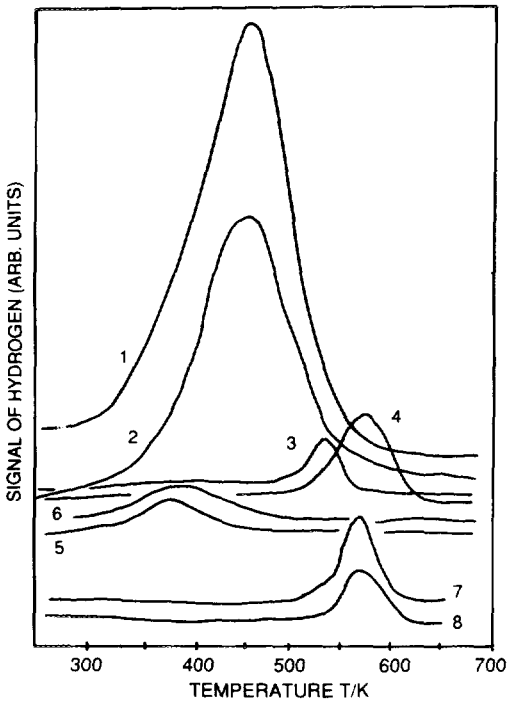

FIG. 6. Temperature-programmed desorption of hydrogen (20 K/min, 32 ml Ar/min): 1—1 wt% Pd/α-Al_2O_3; 2—Pd black; 3—catalyst G (0.5 wt% Pd/ZnO) reduced at 526 K; 4—catalyst G reduced at 643 K; 5—catalyst G desorption after hydrogen titration at 298 K; 6—catalyst D (0.1 wt% Pd/ZnO) desorption after hydrogen titration at 298 K; 7—ZnO hydrogen treated at 493 K; 8—ZnO argon and hydrogen treated at 673 K.

placed by 49.98 Pa H_2 and cooled to 298 K) resulted in peaks at 535 (curve 3) and 575 K (curve 4), respectively. Under these conditions the low temperature peak at 363 K was not observed in either sample. ZnO alone, depending on the temperature of activation, produced peaks at 543–603 K (7 and 8 in Fig. 6). This form of hydrogen always appears after high temperature hydrogen treatment of ZnO as observed by Baranski and Cvetanovic (*19*). ZnO samples hydrogenated at 673 K for two hours and degassed in Ar for 30 min adsorbed 0.56–0.82 μmol/g ZnO at 298 K in 49.98 Pa H_2. After 10 min purging in Ar, 0.32–0.47 μmol hydrogen/g ZnO could be removed at 298 K as indicated by the back adsorption measurements.

For sake of comparison the hydrogen TPD measurements with 1 wt% Pd/α-Al_2O_3 and Pd-black is also depicted (Fig. 6, curves 1 and 2). The peak maxima are in the range of 463–478 K which agrees, considering the differences in heating rates, with the TPD curves measured for Pd/C (*34*).

X-ray Diffraction and DSC

The phase composition of samples C and E has been investigated by X-ray diffraction following TPR measurements in the temperature range 423–873 K. After H_2 treatment at 423 K only Pd and ZnO diffraction lines could be discerned, but at 723 K the formation of a PdZn intermetallic phase (*35*, *36*) with lines at 0.218, 0.207, 0.109, 0.12, 0.167, 0.145, 0.289, and 0.334 nm could be detected (JCPDS 6-620). The diffraction measurements after reduction at 723 and 873 K also indicated weak lines at 0.789, 0.174, 0.158, 0.133 nm, which on the basis of known data (JCPDS 4-883, 6-630, 31-942, 32-723) may be assigned to Pd_5Zn_{21} (JCPDS 4-883 (*35*). Oxidation of the PdZn/ZnO (samples E and F, 8.5 or 4.4 wt% Pd reduced at 673 K for 30 min) above 573 K resulted in separation of the intermetallic phases in accordance with results observed for PdZn (*14*) and PtZn (*12*).

DSC measurements on samples E and F (8.5 or 4.4 w/w% Pd) have shown that bulk oxidation of the intermetallic phase (Fig. 7) is characterized by a peak maximum at about 623 K (heating rate 20 K/min). Bulk oxidation of Pd/α-Al_2O_3 and Pd/SiO_2 (see curve 4) is observed at 523–553 K. The latter values are not far from 580 K proposed by Lam and Boudart (*37*) for full oxidation of small Pd particles.

X-ray Photoelectron Spectroscopy

In situ reduction of sample E (8.5 wt% Pd) was followed by XPS measurements; results are shown in Table 4. The Zn $2p_{3/2}$ binding energy was 1022.0 eV and the O1*s* XPS transition was 530.7 eV in all cases. Even the value of the Zn Auger parameter (α) remained unchanged (2010.3 eV), al-

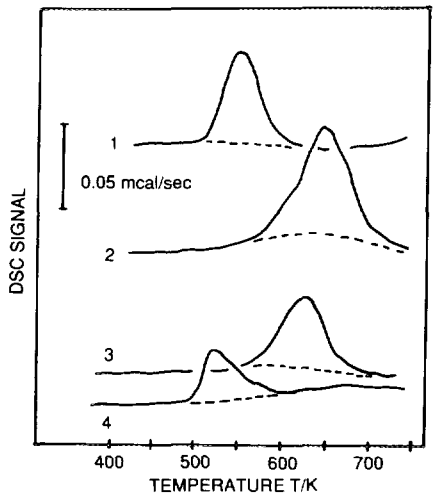

FIG. 7. DSC measurements in air (20 K/min heating rate): 1—catalyst E (8.5 wt% Pd/ZnO); 2—catalyst E reduced at 753 K prior to oxidation; 3—catalyst F (4.4 wt% Pd/ZnO) reduced at 663 K; 4—7.3 Pd/SiO_2.

though on successive reductions an increase of the shoulder in the low binding energy side of the Zn $L_3M_{4,5}M_{4,5}$ Auger peak could be observed. All these results, in agreement with the literature, are characteristic of ZnO reduced slightly upon H_2 treatment (*38, 39*). Other significant features of the reduction are summarized in Table 4. Before reduction, the Pd $3d_{5/2}$ peak was centered at 335.9 eV B.E., indicating palladium ions in +2 valence state. Hydrogenation of the sample at 320 K resulted in a −0.8 eV shift of the Pd $3d_{5/2}$ binding energy as expected for $Pd^{2+} \rightarrow Pd^0$ transformation (*39*). The reduction was also followed by a small increase in the intensity ratio of Pd 3*d*/Zn 2*p* XPS peaks. However, this ratio decreased upon hydrogenation at 520 K without any change in the Pd $3d_{5/2}$ binding energy, which indicates that the Pd^0 particles had increased in size or become decorated with Zn. Upon further increase of the reduction temperature to 670 K, the Pd $3d_{5/2}$ peak was observed to shift 0.8 eV towards higher binding energies as was obtained with Pd on ZnO (*38, 39*) and with other Pd allows (*40*). A simultaneous drop in Pd 3*d*/Zn 2*p* intensity ratio demonstrates a marked decrease in the surface concentration of palladium. The O 1*s*/Zn 2*p* intensity ratio shown in Table 4 decreased monotonously with increasing reduction temperature, providing additional evidence for the growing reduction of Zn^{2+}.

Hydrogenation of 1,3-Butadiene

Conversion of 1,3-butadiene and the selectivity of product formation over ZnO were investigated in a flow reactor with a mixture of 1-butene, 1,3-butadiene, and hydrogen. The results are reported in Table 5. With samples activated in H_2 at 603 K (Series I) or in N_2 at 598 K (Series II), hydrogenation and isomerization activity was detectable from about 373 K. Hydrogenation is not entirely selective, as even in the early stages of the reaction *n*-butane is formed

TABLE 4

XPS Measurements with Sample E (8.5 wt% Pd/ZnO)

Treatment	Zn $2p_{3/2}$ B.E. (eV)[a]	α (Zn) (eV)	Pd $3d_{5/2}$		O 1*s*	
			B.E. (eV)	I_{Pd}/I_{Zn}	B.E. (eV)	I_O/I_{Zn}
As received	1022.0	2010.3	335.9	0.63	530.7	0.39
1 h H_2/320 K	1022.0	2010.3	335.1	0.72	530.7	0.37
1 h H_2/520 K	1022.0	2010.3	335.1	0.64	530.7	0.34
1 h H_2/670 K	1022.0	2010.3	335.9	0.36	530.7	0.29

Note. $\alpha = KE^{Zn}_{Auger} - KE_{2p} + h\nu$, where $h\nu$ = 1486.67 eV and $KE_{Auger} - KE_{2p}$ is the difference between Auger and XPS peak in eV.

[a] Binding energies (B.E.) are referenced to C 1*s* (284.8 eV B.E.).

TABLE 5

Product Selectivity over ZnO

Series	t (min)	T (K)	Conv. (%)[a]	SnB	St2	Sc2	S1B
I	3	378	1.7	0.060	0.441	0.262	0.237
	23	412	4.2	0.033	0.433	0.188	0.346
	45	453	13.1	0.055	0.417	0.175	0.353
	64	473	25.3	0.053	0.584	0.281	0.082
	81	476	23.1	0.050	0.410	0.500	0.040
	112	535	24.7	0.116	0.741	1.007	−0.864
	136	538	27.9	0.102	0.663	0.806	−0.571
	158	533	3.1	0.028	3.990	6.260	−9.278
	188	536	1.2	0.032	6.261	9.644	−14.937
II	12	382	3.3	n.o.	0.230	0.262	0.508
	31	415	3.5	0.011	0.221	0.261	0.507
	55	420	3.6	0.018	0.382	0.328	0.272
	76	431	6.5	0.013	0.384	0.330	0.273
	98	441	6.5	0.013	0.336	0.344	0.307
	123	453	9.2	0.012	0.484	0.548	−0.044
	144	473	27.9	0.019	0.555	0.543	−0.117
	168	472	22.9	0.022	0.573	0.574	−0.169
	190	473	19.3	0.021	0.599	0.618	−0.238
	210	473	17.1	0.015	0.604	0.663	−0.282

Note. Series I, sample treated at 603 K in H_2 for 5 h; series II, sample treated at 598 K in N_2 for 14 h.

[a] Conversion of 1,3-butadiene, SnB, St2, Sc2, and S1B: selectivity of *n*-butane, *trans*-2-butene, *cis*-2-butene, and 1-butene, respectively. Conditions: 0.2 g ZnO, 1.9 v% H_2, 0.25 v% butadiene, 2.25 v% 1-butene, F = 25 ml/min. Reaction temperature was slowly increased and samples were taken periodically. Temperatures shown in column 3 represent those at the time samples were taken.

and 1-butene is isomerized to *cis*- and *trans*-2-butene. Formation of *n*-butane is more pronounced on the hydrogen treated sample. Poisoning of the reaction sites was observed with time on stream at elevated temperatures; as a consequence of poisoning, hydrogenation was inhibited while isomerization of 1-butene still proceeded, which explains the negative selectivity of 1-butene in Table 5.

The Pd/ZnO samples were active for hydrogenation of 1,3-butadiene and 1-butene in the much lower temperature range 273–303 K, but even at those temperatures the hydrogenation activity decreased with time on stream. Preliminary runs indicated that the activity could be stabilized to some extent by subjecting the samples to pulses of butadiene.

In Fig. 8 the product selectivities observed at 298 (sample A) and at 312 K (samples D and G) are depicted. Samples A, D, and G were reduced at 313 K and stabilized at 273 K. With conversion decreased by removing diluted catalyst from the reactor, the selectivity of 1-butene formation increased with the simultaneous decrease of *n*-butane formation. There was also an increase in the trans/cis ratio of 2-butenes, which was above the equilibrium ratio in all cases.

As shown in Fig. 9, hydrogen treatment of the same catalyst samples at 535 K in 99.7 kPa H_2 enhanced 1-butene formation from butadiene and distinctly decreased the selectivity of *n*-butane formation and the rate of hydrogenation. The rates of butadiene consumption on catalysts A, D and G (A was NH_4OH washed) decreased from 4.16×10^{-6}, 6.13×10^{-6}, and 2.11×10^{-5} to 5.33×10^{-8}, 3.14×10^{-7}, and 2.53×10^{-6} mol s^{-1} $gcat^{-1}$, respectively. Rate and se-

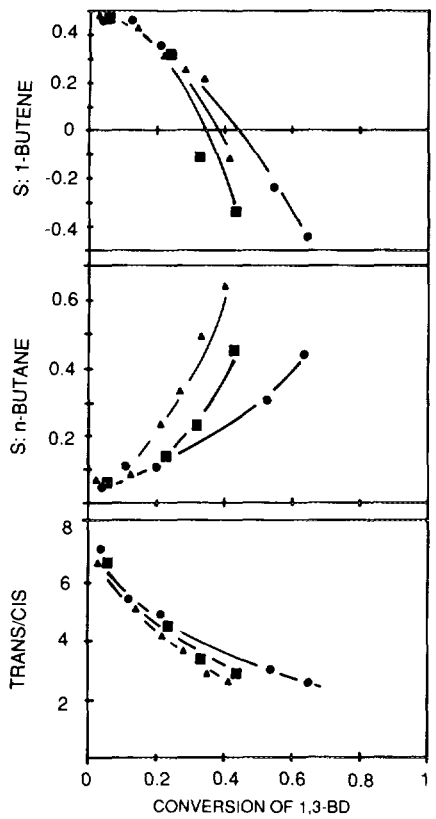

FIG. 8. Hydrogenation of 1,3-butadiene over Catalysts A, D, and G at 298 K (A) and 312 K (D,G). [Inlet composition: 1.9 v% H_2, 0.25 v% 1,3-BD, 2.25 v% 1-B, balance N_2.] ■, Catalyst A; ▲, catalyst D; ●, catalyst G.

lectivity data with sample B are collected in Table 6 for a variety of pretreatment conditions.

The apparent activation energies and reaction orders were determined for butadiene hydrogenation over six Pd/ZnO samples in a batch reactor. These experiments confirmed that the reaction is zero order (0.05+/−0.06) in butadiene and near first order (0.8+/−0.1) in hydrogen. The observed Arrhenius activation energy for butadiene hydrogenation is 65+/−5 kJ/mol. Rates and turnover frequencies (TOFs) are presented in Table 7. The TOFs do not show any significant variation with dispersion but generally increase with the temperature of hydrogen treatment. Product selectivity values are collected in Table 8. Different hydrogen treatments affected the selectivity of 1-butene formation and the trans/cis ratio; both increased as the pretreatment reduction temperature was increased.

DISCUSSION

The TPR and chemisorption results provide clear evidence that the chemisorption and catalytic hydrogenation behavior of Pd/ZnO catalysts can be significantly affected by hydrogen treatment. The results bolster the idea that reduction of the support in presence of Pd is at least partially responsible for the observed effects. Strong reduc-

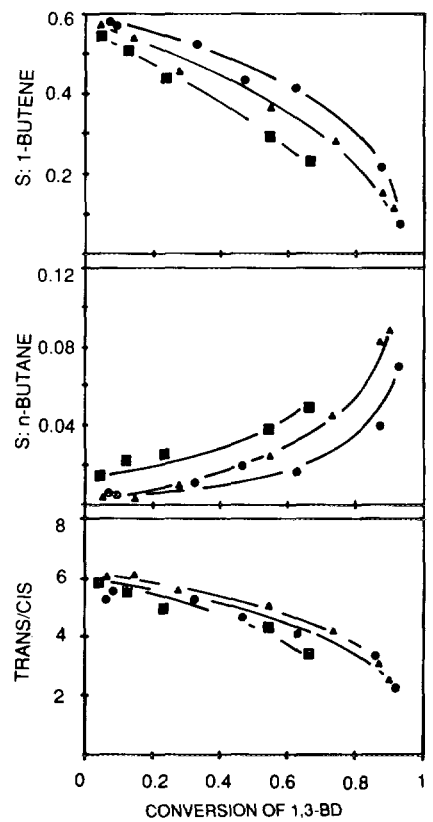

FIG. 9. Hydrogenation of 1,3-butadiene over Catalysts A, D, and G hydrogen treated at 535 K for 30 min. Reaction temp. 310 K. [Inlet composition: 1.9 v% H_2, 0.25 v% 1,3-BD, 2.25 v% 1-B, balance N_2.] ■, Catalyst A; ▲, catalyst D; ●, catalyst G.

TABLE 6

Hydrogenation of Butadiene

Conv. (%)[a]	S1B	St2	Sc2	SnB	*trans*/*cis*
Catalyst B (0.5 Pd/ZnO)					
Sample poisoned by 1,3-BD at 295 K; Rx. T = 327–333 K; $R = 2.2 \times 10^{-6}$ mol s^{-1} gcat^{-1}					
5.7	0.522	0.392	0.053	0.033	7.40
12.3	0.332	0.491	0.146	0.031	3.36
31.3	−0.469	0.910	0.438	0.121	2.08
Hydrogenated at 353 K for 1 h, T = 298 K; $R = 6.4 \times 10^{-6}$ mol s^{-1} gcat^{-1}					
14.8	0.553	0.375	0.061	0.011	6.15
21.5	0.520	0.368	0.100	0.012	3.68
42.2	0.253	0.539	0.184	0.024	2.93
56.6	0.086	0.598	0.227	0.089	2.63
73.6	−0.931	1.247	0.463	0.221	2.69
Hydrogenated at 423 K for 1 h, T = 344–348 K; $R = 3.2 \times 10^{-7}$ mol s^{-1} gcat^{-1}					
10.2	0.591	0.333	0.065	0.011	5.12
34.4	0.578	0.326	0.076	0.020	4.29
66.2	0.511	0.380	0.088	0.021	4.32
73.2	0.488	0.385	0.096	0.031	4.01
81.9	0.436	0.412	0.111	0.041	3.71
91.1	0.163	0.556	0.202	0.079	2.75
Hydrogenated at 473 K for 2 h, T = 343 K; $R = 3.3 \times 10^{-7}$ mol s^{-1} gcat^{-1}					
23.1	0.593	0.315	0.071	0.021	4.44
43.8	0.566	0.332	0.082	0.020	4.05
71.7	0.484	0.389	0.096	0.031	4.05
88.9	0.411	0.426	0.102	0.061	4.18
95.8	0.150	0.503	0.256	0.091	1.96

[a] Conversion of 1,3-butadiene, SnB, St2, Sc2, and S1B: selectivity of *n*-butane, *trans*-2-butene, *cis*-2-butene, and 1-butene, respectively. (Inlet composition: 1.9 v% H_2, 0.25 v% 1,3-BD, 2.25 v% 1-B balanced with N_2.)

tion increases the concentration of Zn^+ (or oxygen deficient sites in the vicinity of the Pd–ZnO interface) and leads to surface decoration of Pd sites by Zn. (Zn+ denotes interstitial zinc atoms whose electrons are thermally excited into the conduction band (*12*, *21*).) From the TPR runs, one sees that hydrogen begins to be consumed from about 333–373 K, which temperature range is definitely lower than those reported by Hong *et al.* (*14*). The weak H_2 TPD signal clearly indicates that the adsorbed hydrogen is being used to reduce ZnO at the higher temperature rather than simply being desorbed. Migration of hydrogen from the Pd particles to the metal-support interface and its consumption by ZnO is faster than desorption from Pd sites. The desorption peak at 533–573, which was observed after reduction treatments at 526 K and 643 K, is probably associated with ZnO (*16*, *18*, *21*); prolonged hydrogenation treatment increases its intensity, but this form of hydrogen could not be removed by O_2 titration at 298 K.

The particle size of Pd plays an important role in the reduction of ZnO and in the subsequent decoration of Pd sites by Zn. As shown in Figs. 4 and 5 for the highly dispersed samples D and G, the $(H/H_0)_s$ values decrease more at lower temperatures than are observed on the less dispersed samples C or E. With catalyst C (not treated with NH_4OH) the hydrogen chemisorption is al-

TABLE 7

Butadiene Hydrogenation: Rates and Turnover Numbers

Catalyst	T (K)[a]	R[b]	H_s[c]	TOF[e]
Circulated batch reactor: 5 kPa BD and 5.1–5.2 kPa H_2; T = 298 K				
A	323	5.31×10^{-6}	3.53×10^{-6}[d]	1.5
A	493	1.23×10^{-7}	1.40×10^{-7}	0.88
A	535	1.49×10^{-7}	7.12×10^{-8}	2.1
B	323	8.23×10^{-6}	5.51×10^{-6}[d]	1.5
B	473	1.40×10^{-7}	2.12×10^{-7}	0.66
C	323	4.21×10^{-5}	2.23×10^{-5}[d]	1.9
C	423	6.69×10^{-6}	6.33×10^{-6}	1.1
C	493	5.85×10^{-6}	2.54×10^{-6}	2.3
C	633	2.06×10^{-6}	5.30×10^{-7}	3.9
D	343	8.95×10^{-5}	6.33×10^{-6}[d]	1.4
D	423	5.51×10^{-6}	1.13×10^{-6}	4.9
D	535	1.26×10^{-6}	2.41×10^{-7}	5.2
G	343	6.37×10^{-5}	2.46×10^{-5}[d]	2.6
G	493	4.33×10^{-6}	1.71×10^{-6}	2.5
G	535	3.91×10^{-6}	7.22×10^{-7}	5.4
G	570	3.81×10^{-6}	5.22×10^{-7}	7.3

[a] Temperature of the reduction treatment.

[b] R in mol/gcat s.

[c] H_s hydrogen chemisorption sites in mol/gcat.

[d] Determined from hydrogen titration, otherwise chemisorption at 293 K after Ar treatment at the temperature of reduction.

[e] Turnover frequency (TOF) in 1/s.

TABLE 8

Hydrogenation of 1,3-Butadiene[a] over Pd/ZnO Catalysts at 298 K

Conv. (%)[a]	SnB	S1B	St2	Sc2	*trans*/*cis*
Catalyst A (0.3 Pd/ZnO) red 535 K; $R = 1.49 \times 10^{-7}$[b]					
3.5	0.0008	0.6312	0.2937	0.0743	3.95
31.9	0.0011	0.5971	0.3182	0.0836	3.81
Catalyst A (0.3 Pd/ZnO) red 323 K; $R = 5.31 \times 10^{-6}$					
7.8	0.0007	0.5922	0.3538	0.0533	6.64
48.3	0.0213	0.5765	0.3446	0.0576	5.98
Catalyst C (2.5 Pd/ZnO) red 633 K; $R = 2.06 \times 10^{-6}$					
11.0	0.0034	0.6455	0.2849	0.0662	4.30
32.4	0.0047	0.6528	0.2741	0.0684	4.01
44.3	0.0055	0.6124	0.2977	0.0844	3.53
Catalyst C (2.5 Pd/ZnO) red 323 K; $R = 4.2 \times 10^{-5}$					
12.3	0.0331	0.5525	0.3633	0.0511	7.11
37.7	0.0452	0.5331	0.3528	0.0689	5.12
Catalyst D (0.1 Pd/ZnO) red 423 K; $R = 5.5 \times 10^{-6}$					
2.8	0.0003	0.6428	0.2967	0.0602	4.93
20.2	0.0011	0.6122	0.3162	0.0705	4.49
34.1	0.0056	0.6130	0.3011	0.0803	3.75
Catalyst G (0.5 Pd/ZnO) red 570 K; $R = 1.91 \times 10^{-6}$					
5.6	0.0001	0.6389	0.2912	0.0698	4.17
17.6	0.0009	0.6437	0.2847	0.0707	4.03
19.5	0.0016	0.5857	0.3256	0.0871	3.74
Catalyst G (0.5 Pd/ZnO) poisoned by 1,3-BD; $R = 3.2 \times 10^{-5}$					
23.8	0.0040	0.5992	0.3436	0.0532	6.46
46.6	0.0042	0.6001	0.3324	0.0633	5.25
Catalyst (0.1 Pd/α-Al_2O_3) poisoned by 1,3-BD; $R = 3.6 \times 10^{-4}$					
11.2	0.0012	0.6043	0.3542	0.0403	8.79
29.9	0.0048	0.6030	0.3322	0.0600	5.54

[a] Batch circulation reactor. Butadiene: 4.9–5.05 kPa, H_2: 5.1–5.2 kPa.
[b] R in mol/gcat s.

most completely suppressed by H_2 treatment above 500 K. The detrimental effect of chlorine was also observed with sample A; NH_4OH treatment after reduction at 393 K increased the chemisorption uptakes. It is likely that $ZnCl^+$ or $ZnCl_2$ present on the surface inhibits chemisorption of hydrogen by physically blocking the Pd sites. The effect of $ZnCl_2$ could also be explained by (i) reduction of $ZnCl_2$ at Pd sites or (ii) poisoning of Pd sites by $ZnCl_2$. Chlorine released during reduction of the Pd precursor remains in the vicinity of Pd particles, and the low melting point of $ZnCl_2$ (556 K) facilitates its migration to and spreading over Pd particles (encapsulation), which renders such surface sites physically unavailable. These effects explain differences among reduction curves 3, 4, and 5 in Fig. 4.

Chemisorption of H_2, O_2, and CO; TPD of H_2; and XPS data support the conclusion that the Pd surface becomes gradually covered by Zn atoms. As shown in Figs. 1–3, at low temperatures ($T < 523$ K) the hydrogen uptake of the Pd_s sites is suppressed more significantly than is the hydride phase formation. These observations are more logically explained by a "skin" model rather than by a continuously progressing front of PdZn intermetallic phase proposed by Hong *et al.* (*14*). At low temperature Zn atoms formed either remain in the vicinity of the Pd–ZnO interface or migrate onto the surface of the Pd particles. On such a surface modified by Zn, some uncovered "portholes" may provide an opportunity for the migration of the hydrogen into the bulk.

Changes in surface composition upon reduction and the effect of particle size are also reflected in the oxygen chemisorption measurements. With both D and G catalysts, hydrogen reduction first increased then decreased the oxygen chemisorption uptakes. For these catalysts the oxygen uptake remains significant even after reduction at 573 K, whereas catalysts B and E exhibited rather limited oxygen uptakes under similar conditions. The difference between O_s(A) and O_s(T) shown in Tables 2 and 3 can be explained by the presence of oxygen vacancies at the metal–support interface or the decoration of Pd by Zn. An interesting feature of our results is that oxygen chemisorption at 298 K on catalysts D and G restores some hydrogen chemisorp-

tion capacity as indicated by the hydrogen titrations. These phenomena point either to the breaking up of Pd–Zn bonds and formation of ZnO islands on Pd particles or to the separation of the Pd–Zn^+ bonds at the metal support interface. As a consequence of the small particle size of Pd, both Zn modified sites and Zn^+ can exist simultaneously on the surface.

With catalysts C and E (dispersions 9 and 2.7%) reduction above 573 K results in very limited chemisorption uptakes which may indicate isolation of Zn on low-index faces of Pd. Such a suggestion is supported by the small oxygen chemisorption at 298 K and by the fact that O_2 uptake at 395–423 K does not ensure formation of Pd_s sites in contrast to observations on the highly dispersed D and G catalysts. Oxidation of PdZn intermetallics formed on catalyst E were observed only at about 623 K in the DSC measurements. At that temperature bulk oxidation of the particles takes place and results in formation of separate Pd and ZnO phases in agreement with results by Hong *et al.* (*14*).

Finally we focus our attention on the catalytic measurements. Product selectivities measured in the atmospheric flow microreactor differ significantly from those observed in static circulation system. The main reason for the enhanced formation of *n*-butane and the rapid decrease of *trans*/*cis* ratio is the large excess of hydrogen used in the flow system. As a consequence of excess hydrogen the coverage of butadiene on the working surface is probably less than that in the case of equimolar H_2/1,3-BD mixtures thereby allowing full hydrogenation and isomerization of butene isomers.

In the static circulation system using H_2/butadiene ratios close to unity, the product selectivity resembles distributions observed generally over Pd (*41–43*). As the pioneering work Wells and Bond (*41, 42*) has established, hydrogenation of 1,3-butadiene on Pd results mostly in the formation of 1-butene and *trans*-2-butene. Moreover, isomerization of alkenes formed is suppressed in the presence of butadiene, and the interconversion between *syn* and *anti* forms of 1,3-butadiene is limited. Thus, *trans*-2-butene is produced by 1,4 addition of hydrogen to the *anti* adsorbed 1,3-butadiene species, while *cis*-2-butene comes from the *syn*-diadsorbed form. *Trans*/*cis* ratios over Pd have been reported to reach values as high as 8.7 (*43*) and 9.7 (*41, 42*) at 313 K. In liquid-phase hydrogenation, Boitiaux *et al.* (*44*) reported a *trans*/*cis* ratio of 12. The large excess of the trans isomer reflects the limited rearrangement of 1,3-butadiene whose adsorbed form probably reflects the gas phase *anti*/*syn* ratio, which is about 19 at room temperature. The TOF values (Table 7) are almost independent of dispersion, as was observed by Boitiaux *et al.* (*45*) in liquid-phase hydrogenation. Massardier *et al.* (*46*) reported a "surface sensitivity" of the reaction, and Tardy *et al.* (*47*) observed a marked decrease of 1,3-butadiene hydrogenation rate for Pd particles in the 3.0–0.8 nm range.

Although dilution of surface Pd sites by Zn drastically reduces the overall rate of 1,3-butadiene hydrogenation, the TOFs are not affected significantly for most samples. However, for catalysts C, D, and E the TOF value definitely increases with more stringent hydrogen treatments. Such an increase may not be directly linked to a hydrogen effect but more likely reflects a decreasing strength of hydrocarbon complexation which increases the rate of hydrogen addition. In zero-order reactions the strength of complexation (adsorption equilibrium constant) disappears from the intrinsic Langmuir–Hinshelwood rate equation.

The changes in the product selectivity can be interpreted by considering two controlling factors: first, there is a limited concentration of surface hydrogen on Zn decorated Pd sites; second, the concentration of sites which allows adsorption and competition between 1,3-butadiene and 1-butene has changed.

n-Butane formation, which occurs read-

ily on fresh samples with the typical inlet composition of 1.9 v% H_2, 0.25 v% butadiene, and 2.25 v% 1-butene, is significantly decreased upon reduction treatments at 493 K. The suppression of complete saturation is in accordance with the very limited hydrogen chemisorption capacity of the Zn decorated Pd particles. Without Zn decoration, as shown by Fig. 8 and Table 6, the selectivity of 1-butene becomes negative even at moderate conversions which means that 1-butene is consumed from the reaction mixture. Since at 413 K 2-butenes are thermodynamically favored over 1-butene by a factor of 20/1, in the absence of butadiene on the surface 1-butene readily isomerizes to 2-butenes. On Zn-modified samples there is a net production of 1-butene, but the isomerization to *cis*- and *trans*-2-butenes is not entirely blocked. Even at low conversions the *cis*-2-butene/*trans*-2-butene ratio is somewhat less than values reported on Pd catalysts. The change of the *cis*/*trans* ratio was also observed without 1-butene added, i.e., under conditions when the surface is covered almost exclusively with 1,3-butadiene. We attribute this effect to limited interconversion between the *syn* and *anti* form of 1,3-butadiene allowing change in conformation of adsorbed 1,3-butadiene. The weaker interaction of 1,3-butadiene with Zn-modified Pd allows some reversibility in the hydrogenation steps which on Pd, because of the strong complexation of butadiene, are almost irreversible.

One cannot entirely rule out some isomerization on Zn^+ sites or some intervention of Pd–Zn^+ pair sites. Although the hydrogenation activity of ZnO is extremely low, its basicity permits dissociation and isomerization of butenes (*20*). The number of reactive sites on ZnO depends significantly on pretreatment conditions. Upon hydrogen treatment of Pd/ZnO, the Pd sites become less active, which could result in relatively more reaction occurring on the support sites. It is also possible that hydrogen spillover during high temperature reduction could produce a higher concentration of active sites than are observed under the usual pretreatments in vacuum or inert gas. Acidic sites on Pd/TiO_2 (*48*), Pd supported on La_2O_3, CeO_2, Pr_6O_{11}, Nd_2O_3 (*49*), and Pd/TiO_2 modified by WO_3 (*50*) have also been shown to increase the rate of hydrogenation and the rate of double bond shift. Further work is necessary with Pd/ZnO systems to separate Zn^+ and Pd/Zn effects.

CONCLUSIONS

Hydrogen treatment of Pd/ZnO samples results in the formation of oxygen-deficient sites at the Pd–ZnO interface and leads to Zn decorated Pd particles. The chemisorption of hydrogen decreases faster than its absorption upon high-temperature hydrogen treatments indicating rapid surface migration of Zn. Oxidation of decorated Pd particles (dispersion 78 and 64%) at 293 K restores to some extent the hydrogen chemisorption activity. X-ray diffraction, XPS, and volume hydrogen consumed in reduction confirm formation of a PdZn intermetallic phase at elevated temperatures. The presence of chlorine in the palladium precursor affects the surface composition as the chlorine remains attached to Zn^{2+} and leaves the system only by sublimation as $ZnCl_2$.

The selectivity of hydrogenation of 1,3-butadiene in 1-butene increases upon hydrogen treatment from about 423 K with a simultaneous decrease of the catalyst activity. Formation of *n*-butane is retarded as a consequence of the limited surface coverage of hydrogen. The variation of *trans*/*cis* ratios observed at low conversions points to interconversion of *syn* and *anti* conformations of adsorbed 1,3-butadiene on PdZn or participation of acid–base pairs in the isomerization processes. An increase in the TOF upon reduction treatment might be attributed to a weaker interaction of 1,3-butadiene with Zn-modified sites.

ACKNOWLEDGMENTS

This work was financially supported by the NSF International Division (INT-8807331), Hungarian

Academy of Sciences, and partly from the Grant OTKA 1887.

REFERENCES

1. Schwab, G. M., *Adv. Catal.* **27,** 1 (1978).
2. Solymosi, F., *Catal. Rev.* **1,** 233 (1967).
3. Tauster, S. J., Fung, S. G., and Garten, R. L., *J. Am. Chem. Soc.* **100,** 170 (1978).
4. Ponec, V., "Metal Support and Metal Additive Effects in Catalysis" (B. Imelik *et al.*, Eds.), p. 3. Elsevier, Amsterdam, 1982.
5. Haller, G. L., and Resasco, D. E., *Adv. Catal.* **36,** 173 (1989).
6. Ichikawa, M., Lang, A. J., Shriver, D. F., and Sachtler, W. M. H., *J. Am. Chem. Soc.* **107,** 7216 (1985).
7. Jen, H. W., Zheng, Y., Shriver, D. F., and Sachtler, W. M. H., *J. Catal.* **116,** 361 (1989).
8. Ghorai, D. K., Sanyal, R. M., Sen, B., Ghosh, S. K., Banerji, E. S., Shapiro, E. S., and Minachev, Kh. M., *React. Kinet. Catal. Lett.* **40,** 259 (1989).
9. Wehner, P. S., Mercer, P. N., and Apai, G., *J. Catal.* **84,** 244 (1983).
10. Ichikawa, M., *Bull. Chem. Soc. Jpn.* **51,** 2268, 2273 (1978).
11. Li, W., Chen, Y., Yu, C., Wang, X., Hong, Z. and Wei, Z., *in* "Proceedings, 8th International Congress on Catalysis, Berlin, 1984," Vol. 5, p. 205. Dechema, Frankfurt am Main, 1984.
12. Boccuzzi, F., Chiorino, A., Ghiotti, G., Pinna, F., Strukul, G., and Tessari, R., *J. Catal.* **126,** 381 (1990).
13. Boccuzzi, F., Ghiotti, G., Chiorino, A., and Marchese, L., *Surf. Sci.* **233,** 141 (1990).
14. Hong, C. T., Yeh, C. T., and Yu, F. H., *Appl. Catal.* **48,** 385 (1989).
15. Rylander, P. N., "Catalytic Hydrogenation in Organic Syntheses," p. 72. Academic Press, New York, 1979.
16. Kokes, R. J., and Dent, A. L., *Adv. Catal.* **22,** 1 (1972).
17. Bozon-Verduraz, F., and Teichner, S. J., *J. Catal.* **11,** 7 (1968).
18. Dent, A. L., and Kokes, R. J., *J. Am. Chem. Soc.* **92,** 1092, 6709, 6718 (1970).
19. Baranski, A., and Cvetanovic, R. J., *J. Phys. Chem.* **75,** 208 (1971).
20. Dent, A. L., and Kokes, R. J., *J. Phys. Chem.* **75,** 487 (1971).
21. Scholten, J. J. F., and van Montfoort, A., *in* "Proceedings, 5th International Congress on Catalysis, Palm Beach, 1972" (J. W. Hightower, Ed.), p. 385. North-Holland, Amsterdam, 1973.
22. Tuley, W. F., and Adams, R., *J. Am. Chem. Soc.* **45,** 3061 (1925).
23. Naidin, V. A., Zakumbaeva, G. D., and Sokolskii, D. V., *Katal. Reacts. Zhidk. Faze* **417** (1972); *Chem. Abstr.* **79,** 115042p (1973).
24. Boitiaux, J. P., Cosyns, J., and Martino, G., *in* "Metal Support and Metal Additive Effects in Catalysis" (B. Imelik *et al.*, Eds.), p. 355. Elsevier, Amsterdam, 1982.
25. Boitiaux, J. P., Cosyns, J., and Vasudevan, S., *Appl. Catal.* **15,** 317 (1985).
26. Derrien, M. L., *in* "Catalytic Hydrogenation" (L. Cerveny, Ed.), p. 613. Elsevier, Amsterdam, 1986.
27. Guczi, L., and Schay, Z., *in* "Catalytic Hydrogenation" (L. Cerveny, Ed.), p. 313. Elsevier, Amsterdam, 1986.
28. Blanchard, G., Charcosset, H., Forissier, M., Matray, F., and Tournayan, L., *J. Chromatogr. Sci.* **20,** 369 (1982).
29. Sermon, P. A., *J. Catal.* **24,** 460 (1972); 24, 467 (1972).
30. Benson, J. E., Hwang, H. S., and Boudart, M., *J. Catal.* **30,** 146 (1973).
31. Boudart, M., and Hwang, H. S., *J. Catal.* **39,** 44 (1975).
32. Riley, M. G., Ph.D. thesis, Rice University, Houston, 1989.
33. Hightower, J. W., Furlong, B., Sarkany, A., and Guczi, L., 10th International Congress on Catalysis, Budapest, 1992, Poster no. 235.
34. Konvalinka, J. A., and Scholten, J. J. F., *J. Catal.* **48,** 374 (1977).
35. Pearson, W. B., *in* "Handbook of Lattice Spacings and Structures of Metals and Alloys" (G. V. Raynor, Ed.), Monographs on Metal Physics and Physical Metallurgy, Vol. 4, p. 814. Pergamon Press, London, 1958.
36. Nowotny, H., and Bittner, H., *Mh. Chem.* **81,** 679 (1950).
37. Lam, Y. L., and Boudart, M., *J. Catal.* **47,** 393 (1977).
38. Wehner, P. S., Tustin, G. C., and Gustafson, B. L., *J. Catal.* **88,** 246 (1984).
39. Zsoldos, Z., and Sarkany, A., in preparation.
40. Steiner, P., and Hufner, S., *Solid State Commun.* **41,** 619 (1982).
41. Bond, G. C., and Wells, P. B., *Adv. Catal.* **15,** 91 (1964).
42. Webb, G., *in* "Catalytic Hydrogenation in Comprehensive Chemical Kinetics" (C. H. Bamford and C. F. H. Tipper, Eds.), Vol. 20, p. 1. Elsevier, Amsterdam, 1978.
43. Meyer, E. F., and Burwell, R. L., *J. Am. Chem. Soc.* **85,** 2281 (1963).
44. Boitiaux, J. P., Cosyns, J., and Robert, E., *Appl. Catal.* **35,** 193 (1987).
45. Boitiaux, J. P., Cosyns, J., and Robert, E., *Appl. Catal.* **32,** 145 (1987).
46. Massardier, J., Bertolini, J. C., and Renouprez, A., *in* "Proceedings, 9th International Congress on Catalysis, Calgary, 1988 (M. J. Phillips and M. Ternan, Eds.), Vol. 3, p. 1222. Chem. Inst. Canada, Ottawa, 1988.

47. Tardy, B., Noupa, C., Leclercq, C., Bertolini, J. C., Hoareau, A., Treilleux, M., Faure, J. P., and Nihoul, G., *J. Catal.* **129,** 1 (1991).
48. Vannice, M. A., and Chou, P., *in* "Proceedings, 8th International Congress on Catalysis, Berlin, 1984," Vol. 5, p. 99. Dechema, Frankfurt am Main, 1984.
49. Mitchell, M. D., and Vannice, M. A., *Ind. Eng. Chem. Fundam.* **23,** 88 (1984).
50. Stadler, K. H., Schneider, M., and Kochloefl, K., *in* "Proceedings, 8th International Congress on Catalysis, Berlin, 1984," Vol. 5, p. 229. Dechema, Frankfurt am Main, 1984.